

Design Method for a $\Sigma\Delta$ -Based Closed Loop Gyroscope

Ahmed K. El-Shennawy
Si-Ware Systems
Cairo, Egypt
ahmed.elshennawy@si-ware.com

Hassan Aboushady
University of Pierre and Marie Curie
Paris, France
Hassan.Aboushady@lip6.fr

Ayman El-Sayed
Si-Ware Systems
Cairo, Egypt
ayman.elsayed@si-ware.com

Abstract—In this paper, we present a design method for a $\Sigma\Delta$ -based closed loop gyroscope. The design is based on the equivalence between electro-mechanical $\Sigma\Delta$ noise transfer function and the noise transfer function of conventional electrical $\Sigma\Delta$. The method is applied to a fourth-order electro-mechanical $\Sigma\Delta$ containing the gyroscope and a second order electrical filter. The noise and signal transfer functions as well as the stability of the designed electro-mechanical $\Sigma\Delta$ are analyzed. Simulation results of the closed loop $\Sigma\Delta$ -based gyroscope measuring the signal-to-noise ratio are given and compared with the corresponding electrical modulator.

I. INTRODUCTION

Micro-machined gyroscopes for measuring rate or angle of rotation have attracted a lot of attention during the past few years for several applications. They can be used as a low-cost miniature companion with micro-machined accelerometers to provide heading information for inertial navigation purposes, for ride stabilization and rollover detection in automotive applications; in some consumer electronic applications, such as video-camera stabilization. Conventional rotating wheel as well as precision fiber-optic and ring laser gyroscopes are all too expensive and too large for use in most emerging applications. Micro-machining can shrink the sensor size by orders of magnitude, reduce the fabrication cost significantly, and allow the electronics to be integrated on the same silicon chip.

Embedding the gyroscope in a closed loop architecture achieves relatively larger bandwidth especially with high Q resonators, improves its linearity and its dynamic range. Different solutions have been suggested in the literature for gyroscope closed loop architecture, [1]–[5] only the first one is an all digital control loop and the rest are electro-mechanical $\Sigma\Delta$ loops. Setting up the control loop as a $\Sigma\Delta$ modulator is convenient in conversion of input force to digital reading with high resolution; this eliminates the need of a separate high resolution ADC.

Fig. 1 shows a closed loop architecture implemented as an electro-mechanical $\Sigma\Delta$ modulator. The gyroscope modeled as a second order resonator is embedded in the loop filter of the modulator and the electrical filter can be simply a lead compensation, this forms a second order modulator. The second order electro-mechanical $\Sigma\Delta$ has a limited resolution, a higher order $\Sigma\Delta$ modulator is needed for higher resolution

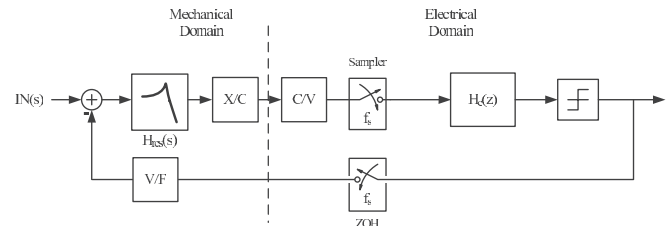


Fig. 1. Electro-Mechanical $\Sigma\Delta$ Modulator

[6]. This can be done by including additional electrical filters in the loop.

Stabilizing the electro-mechanical $\Sigma\Delta$ modulator is a challenge compared to an electrical one; modeling the gyroscope as a second order system, we have only access to the resonator output. The output of the first integrator is not accessible and a phase-lag is introduced in the loop [7] and a zero is missed to compensate the loop. In [6], the authors suggest the addition of a lead compensation and in [7], the authors suggest replacing the front-side resonator stage of an electrical $\Sigma\Delta$ modulator with the mechanical sensor in such a way that the output of the first integrator is not needed.

In this work, a design method for a high order electro-mechanical $\Sigma\Delta$ is presented. The design is based on equivalence between the loop filter of typical electrical $\Sigma\Delta$ modulator and the loop of filter of the electro-mechanical $\Sigma\Delta$ modulator applying the procedure in [8] focusing on the coefficients calculation of the electrical filter. The proposed design method achieves a good performance in terms of stability and quantization noise shaping. A design example is presented based on a fourth order feedforward architecture using linear models and verified by transient simulations.

The paper is organized as follows. In Section II, we present the methodology of designing a closed loop solution for gyroscope using an electro-mechanical $\Sigma\Delta$. In Section III, we present a design example of a fourth order modulator and its simulations results and we finally end with conclusion in Section IV.

II. CLOSED LOOP DESIGN

A. A Discrete Time Quasi-Linear Loop Model

The design process of closed loop solution using electro-mechanical $\Sigma\Delta$ architecture is done in the discrete time

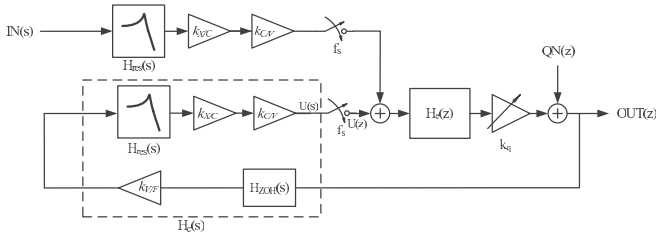


Fig. 2. Quasi linear model of the modulator

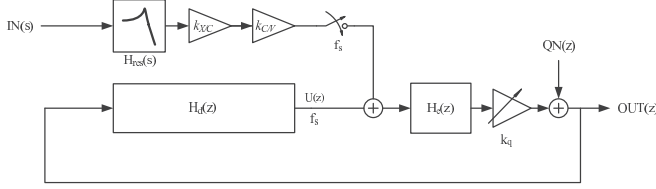


Fig. 3. Discrete Time Quasi-Linear Loop Model

domain using a quasi-linear model of the loop. This model is used in the next section while designing the electrical filter. Linearizing all functions in the loop is done around the rest position (zero input); these functions are the voltage-to-force linearized to $k_{V/F}$ ignoring non-linearities in the actuators, displacement-to-capacitance linearized to $k_{X/C}$ and capacitance-to-voltage linearized to $k_{C/V}$ assuming linear conversion in both. The comparator is replaced by a variable gain k_q and additive white noise $QN(z)$ modeling the quantization noise [9]. The mechanical resonator is modeled by

$$H_{res}(s) = \frac{1/(m\omega_0^2)}{s^2 + \frac{1}{\omega_0 Q}s + 1} \quad (1)$$

where m is the mass, Q is the quality factor and $(\omega_0/2\pi)$ is the resonance frequency. And the zero order hold (ZOH) in the feedback is modeled by

$$H_{ZOH}(s) = \frac{(1-e^{-sT_s})}{s} \quad (2)$$

where T_s is the sampling period.

Fig. 1 shows the electro-mechanical $\Sigma\Delta$ loop block diagram and Fig. 2 shows its quasi-linear model. In Fig. 2, the continuous time signal path is broken up from the discrete time signal path, this is used while studying the noise transfer function NTF and the signal transfer function STF . From Fig. 2, we can define $H_c(s)$ as

$$H_c(s) = k_c \frac{(1-e^{-sT_s})}{s(\frac{s^2}{\omega_0^2} + \frac{1}{\omega_0 Q}s + 1)} \quad (3)$$

$$k_c = -\frac{k_{V/F}k_{X/C}k_{C/V}}{m\omega_0^2}$$

By applying the z-transform, we can define $H_d(z)$ as the discrete-time transfer function of the output signal $OUT(z)$ to the sampled C/V output $U(z)$

$$H_d(z) = \frac{U(z)}{OUT(z)} = z \{H_c(s)\} = k_d \frac{(z-z_m)}{(z-p_m)(z-p_m^*)} \quad (4)$$

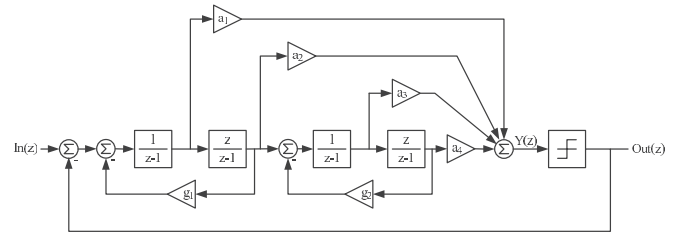


Fig. 4. Electrical $\Sigma\Delta$ 4th order feedforward modulator

where the discrete time complex poles (p_m and p_m^*) are located at $\omega_0/2\pi$, the discrete-time zero z_m is mapped from the ZOH, while k_d is a gain coefficient and it is a function of k_c and the sampling frequency f_s . Fig. 3 shows the discrete-time quasi-linear loop model with continuous time signal path of the input signal.

Using the model in Fig. 3, the output ($OUT(z)$) is found to be

$$OUT(z) = \frac{M(s)H_e(z)}{1-k_q LG(z)} IN(s) + \frac{1}{1-k_q LG(z)} QN(z) \quad (5)$$

where

$$M(s) = k_{X/C}k_{C/V}H_{res}(s) \quad (6)$$

$$LG(z) = H_d(z)H_e(z)$$

then consequently NTF and STF of the electro-mechanical $\Sigma\Delta$ modulator (NTF_{em} and STF_{em}) are obtained as following

$$NTF_{em}(z) = \frac{1}{1-k_q LG(z)}$$

$$STF_{em}(j\omega) = \frac{M(s)H_e(e^{j\omega})}{1-k_q LG(e^{j\omega})} \quad (7)$$

B. Coefficient Calculations of Electronic Filter

Using the method in [8], an equivalence between NTF_{em} of (7) and a reference discrete-time NTF (NTF_{ref}) of a conventional integrator-based $\Sigma\Delta$ designed using [10] is done. Assuming k_q equal to one and using (7), we get

$$H_d(z)H_e(z) = 1 - \frac{1}{NTF_{em}(z)} = 1 - \frac{1}{NTF_{ref}(z)} \quad (8)$$

Since it is not possible to modify the parameters of the mechanical resonator, $H_{res}(s)$, and consequently $H_d(z)$ the NTF equivalence is performed using the coefficients of the discrete-time electrical filter $H_e(z)$.

III. DESIGN EXAMPLE

Here, the design of a fourth order electro-mechanical $\Sigma\Delta$ modulator is illustrated based on a conventional electrical fourth order $\Sigma\Delta$ modulator built using a feedforward topology (Fig. 4). Utilizing [10], NTF_{ref} is designed to locate one of its complex pair zeros at the resonance frequency of the mechanical zero, $\omega_0/2\pi$.

Same as (8), we can get

$$LG_{ref}(z) = 1 - \frac{1}{NTF_{ref}(z)} = K_{ref} \frac{(z-z_r)(z-z_c)(z-z_c^*)}{(z-p_m)(z-p_m^*)(z-p_e)(z-p_e^*)} \quad (9)$$

$$= K_{ref} \frac{(z-z_r)(z^2-2\text{Re}(z_c)z+|z_c|^2)}{(z-p_m)(z-p_m^*)(z-p_e)(z-p_e^*)}$$

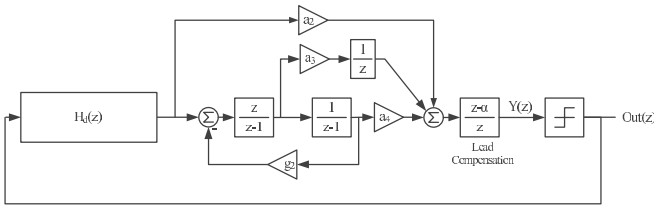


Fig. 5. Fourth order Electro-Mechanical $\Sigma\Delta$ modulator based on a feedforward topology with a lead compensation for loop stabilization [6]

where LG_{ref} is the reference loop gain transfer function, K_{ref} is a gain coefficient, p_m and p_m^* are poles located at $\omega_0/2\pi$, p_e and p_e^* are additional poles added by the electrical resonator and z_r , z_c and z_c^* are zeros needed for loop compensation. LG_{ref} is used in coefficients calculations of the electro-mechanical loop gain transfer function LG_{em} .

In this paper, [6] is taken as a reference design for implementing a closed loop solution. The suggested electro-mechanical $\Sigma\Delta$, shown in Fig. 5, is a fourth order modulator based on a feedforward topology with a lead compensation for loop stabilization. From Fig. 5, LG_{em} is derived

$$LG_{em} = K_{em} \frac{(z-z_m)}{(z-p_m)(z-p_m^*)} \cdot \frac{z-\alpha}{z} \cdot \frac{a_2 z^2 + (a_2(g_2-2) + a_3 + a_4)z + (a_2 - a_3)}{(z^2 - (2-g_2)z + 1)} \quad (10)$$

Equivalence between LG_{ref} and LG_{em} is done by equating numerators and denominators of both. Since we are using single feedback architecture, mismatch between K_{ref} and K_{em} is not important as it is compensated by the comparator in the loop. Ignoring the mechanical zero z_m and the pole at the origin for the moment one can obtain

$$\begin{aligned} g_2 &= 2(1 - \text{Re}(p_e)) \\ \alpha &= z_r \\ a_2 &= 1 \\ a_3 &= -|z_c|^2 + a_2 \\ a_4 &= -2\text{Re}(z_c) - (a_2(g_2 - 2) + a_3) \end{aligned} \quad (11)$$

TABLE I
LOOP PARAMETERS AND COEFFICIENTS OF A FOURTH ORDER ELECTRICAL $\Sigma\Delta$ MODULATOR AND ITS CORRESPONDING ELECTRO-MECHANICAL $\Sigma\Delta$ MODULATOR

	Electrical	Electro-Mechanical
f_s	500 kHz	
Q	-	1e4
$\omega_0/2\pi$	-	4 kHz
a_1	0.4593	-
a_2	0.1527	1
a_3	0.0254	0.1333
a_4	0.0020	0.0267
g_1	0.0023	-
g_2	0.0025	0.0025
α	-	0.8659

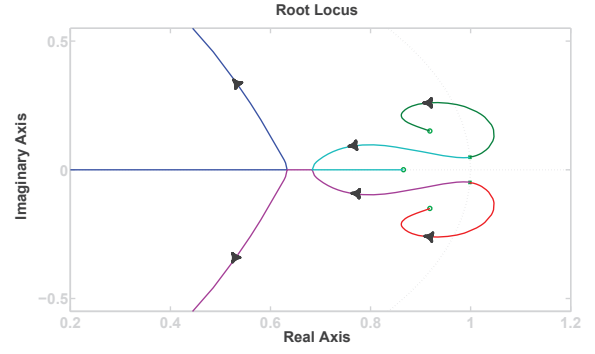


Fig. 6. Root locus of Electro-Mechanical $\Sigma\Delta$ varying k_q

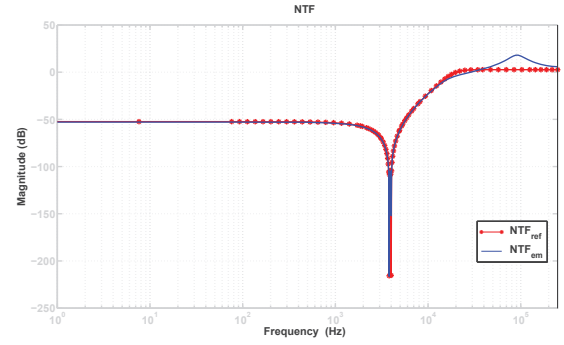


Fig. 7. Noise transfer function of electrical modulator versus electro-mechanical

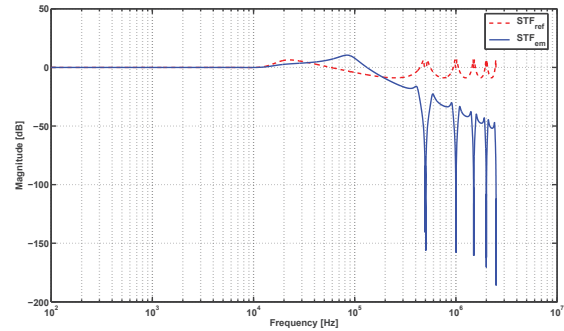


Fig. 8. Signal transfer function of electrical modulator versus electro-mechanical

These calculated coefficients are used while studying the stability of the loop and the performance of the designed modulator. Table I lists the loop parameters and coefficients of a conventional feedforward modulator given by [10] with the coefficients of its corresponding electro-mechanical modulator calculated using the proposed method.

A. Stability, NTF and STF

Studying the stability of the loop while varying k_q , the root locus of the resulting Electro-Mechanical $\Sigma\Delta$ loop (Fig. 6) shows stable operation of the closed loop solution based on the calculated coefficients and with the presence of an extra pole at the origin and the mechanical zero. This stable operation is guaranteed for certain range of k_q , this range is enough for a

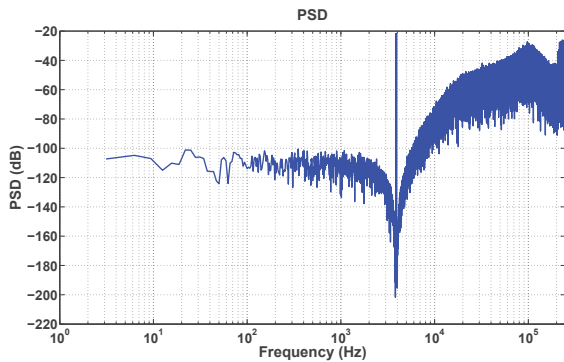


Fig. 9. Power spectral density of Electro-Mechanical $\Sigma\Delta$ with $200^\circ/s$ input

large input stable range.

Using (7) and assuming k_q equal to one, the NTF_{em} and the STF of the electro-mechanical modulator (STF_{em}) is compared to NTF_{ref} and the STF_{ref} of the conventional feedforward electrical modulator (Fig. 7-8). In the previous calculations, an approximation is done by canceling the origin pole and the mechanical zero. The impact of this approximation is the addition of phase lag in the loop which leads to a reduction in its phase margin. This reduction causes peaking in the NTF_{em} as shown in Fig. 7, and it is translated in a reduction in maximum input stable range of the electro-mechanical modulator relative to an electrical one.

Fig. 8 shows a large bandwidth compared to an open loop architecture with a high Q resonators, the signal band centered at $3.95kHz$ is flat. An important difference between STF_{em} and STF_{ref} is the second order filtering of the mechanical resonator in the electro-mechanical modulator which acts as an AAF (Anti-Aliasing Filter).

B. Simulations Results

In order to validate the loop design, a time domain model of the electro-mechanical sigma delta is built and simulated in Matlab. Table I contains the loop parameters used in simulations. Fig. 9 shows the PSD of the modulator output with an angular rate equal to $200^\circ/s$ (-16 dBFS) is used as an input to the loop. As expected from the root locus, a stable operation of the loop is obtained and the quantization noise shaping is the same as the calculated NTF_{em} of the quasi-linear model and the calculated signal to quantization noise ratio (SQNR) is 127 dB for a 200 Hz bandwidth.

A valuable simulation is to test the input stable range of the fourth-order electro-mechanical $\Sigma\Delta$ modulator and its equivalent fourth-order electrical $\Sigma\Delta$ modulator. Fig. 10 shows the SNR versus the input amplitude of both modulators, the electro-mechanical modulator has 4 dB lower input stable range due to the peaking at the NTF_{em} near $f_s/2$.

IV. CONCLUSION

A design method for a $\Sigma\Delta$ -based closed loop gyroscope is presented. The method is applied to a fourth-order electro-mechanical $\Sigma\Delta$ containing the gyroscope and a second order

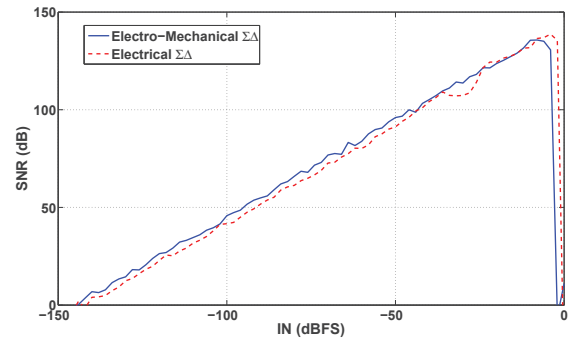


Fig. 10. SNR vs input amplitude for the 4th order electro-mechanical $\Sigma\Delta$ modulator and its equivalent 4th order electrical $\Sigma\Delta$ modulator.

electrical filter. First, loop coefficients are calculated using the equivalence with a conventional electrical $\Sigma\Delta$ modulator. Next, loop stability is studied using quasi-linear model. Finally the stable operation and the closed loop performance is examined using time domain simulations. The electro-mechanical modulator achieves high SQNR as conventional electrical modulator and a comparable input stable range.

ACKNOWLEDGMENT

The authors would like to thank Si-Ware Systems for supporting this research. The help of M.El-Badry, A.Safwat and A.Shaban is greatly appreciated. They also thank Botros George for many helpful discussions.

REFERENCES

- [1] H. Rodjegard, D. Sandstrom, P. Pelin, N. Hedenstierna, D. Eckerbert, and G. Andersson, "A digitally controlled mems gyroscope with 3.2 deg/hr stability," in *Tech. Digest, TRANSDUCERS'05*, Seoul, Korea, 2005, p. 535538.
- [2] J. I. Seeger, X. Jiang, M. Kraft, and B. E. Boser, "Sense finger dynamics in a sd force-feedback gyroscope," in *Proc. IEEE Solid-State and Actuator Workshop*, Hilton Head Island, 2000, p. 296299.
- [3] J. Raman, E. Cretu, P. Rombouts, and L. Weyten, "A closed-loop digitally controlled mems gyroscope with unconstrained sigma-delta force-feedback," *IEEE Sensors Journal*, vol. 9, no. 12, pp. 297–305, March 2009.
- [4] M. Dienger, A. Buhmann, T. Northemann, T. Link, and Y. Manoli, "Low-power continuous-time sigma-delta interface for micromachined gyroscopes employing a sub-nyquist-sampling technique," in *Tech. Digest, TRANSDUCERS 07*, Lyon, France, 2007, p. 1179–1182.
- [5] Y. Dong, M. Kraft, and W. Redman-White, "Micromachined vibratory gyroscopes controlled by a high-order bandpass sigma-delta modulator," *IEEE Sensors Journal*, vol. 7.
- [6] V. P. Petkov and B. E. Boser, "A fourth-order sigma delta interface for micromachined inertial sensors," *IEEE Solid-State Circuits Journal*, vol. 40, no. 8, pp. 1602–1609, Aug. 2005.
- [7] J. Raman, P. Rombouts, and L. Weyten, "An unconstrained architecture for high-order sigma delta force-feedback inertial sensors," in *ISCAS07, IEEE Int. Symp. Circuits Syst.*, New Orleans, LA, USA, May 2007, pp. 3063–3066.
- [8] H. Aboushady and M. Louerat, "Systematic approach for discrete-time to continuous-time transformation of sigma-delta modulators," in *ISCAS02, IEEE Int. Symp. Circuits Syst.*, Phoenix, AZ, USA, May 2002, pp. IV–229 – IV–232.
- [9] R. Schreier and G. C. Temes, *Understanding Delta-Sigma Data Converters*. John Wiley & Sons, Inc., 2005.
- [10] R. Schreier, "The delta-sigma toolbox for matlab oregon state university," Nov. 1999. [Online]. Available: <http://www.mathworks.com/matlabcentral/fileexchange/>